UCRL-5195 Rev.

UNIVERSITY OF CALIFORNIA

Lawrence Radiation Laboratory

Livermore, California

Contract No. W-7405-eng-48

BOUNDARY-LAYER FORMATION IN THE PINCH

John Killeen, Gordon Gibson, and S. A. Colgate

August 10, 1959

Printed for the U.S. Atomic Energy Commission

UCRL-5195 Rev.

Boundary-Layer Formation in the Pinch*

John Killeen, Gordon Gibson,† and S. A. Colgate

Lawrence Radiation Laboratory, University of California
Livermore, California

ABSTRACT

A study is made of various processes that occur prior to the pinch effect when an electric field is applied to a deuterium gas. The variables of the problem are the percentage of ionization, the electron and ion temperatures, the resistivity of the gas, and the current density. A one-dimensional problem is considered in which the above variables are determined as functions of one space dimension and the time. The equations determining these variables are: the heat developed as the current flows through the gas equals the rate of increase of the internal energy of the plasma, the equation describing the rate of ionization, the equation describing the rate of transfer of energy from electrons to ions and the electromagnetic field equations. These equations are a generalization of the plasma equations solved in the paper of Wyld and Watson[1] in that spatial dependence is included, i.e., a current layer is calculated instead of assuming a constant current. The equations are solved numerically using an IBM 704 computer.

---

*Work performed under auspices of the U.S. Atomic Energy Commission.

†Visiting from Westinghouse Atomic Power Department, Pittsburgh, Penna.

[1]N. W. Wyld and K. M. Watson, "Ionization and Heating of a Plasma in a Magnetic Field," Conference on Controlled Thermonuclear Reactions, June 4-7, 1956, Gatlinburg, Tennessee, U.S. Atomic Energy Commission, Division of Research, Controlled Thermonuclear Branch, Report No. TID-7520(Pt. 2), September 1956.

Boundary-Layer Formation in the Pinch

John Killeen, Gordon Gibson, and S. A. Colgate

Lawrence Radiation Laboratory, University of California

Livermore, California

I. INTRODUCTION

Containment of plasmas may be achieved by either vacuum magnetic fields or pinch magnetic fields. Vacuum magnetic fields are created by external coils, whereas in the pinch device the primary current is induced in the plasma, and without this current no containing field exists. The current and magnetic field spatial distributions are of interest since the degree of stability of the pinch plasma column is dependent on the sharpness of the boundary.

In this paper processes that determine the pinch current's spatial distribution for times prior to the implosion of a deuterium plasma are examined. A one-dimensional problem is treated where there is an externally applied stabilizing magnetic field in the direction of the electric field which immobilizes the charged particles in the plasma. It is assumed that this field is of such a magnitude as to make the heat and charged particle diffusion terms across the field negligible. In this manner, wall effects are also conveniently eliminated. Further, the strength of the self or pinching magnetic field (component of the magnetic field normal to the electric field) is considered to be small relative to the stabilizing magnetic field over the interval of time for which the results are significant. Hence, mass motion of the plasma is ignored. As a result of these assumptions, the stabilizing field does not appear explicitly in the calculation. The validity of these assumptions is examined in the discussion of the results.

The plasma equations of Wyld and Watson[1] are generalized to include spatial dependence. The different particles are treated as having local Maxwellian distributions, i.e., temperatures are assigned. This is a limitation on this work, since for the particle densities and electric field strengths utilized in pinch work some electrons should tend to "run-away." However, should this effect result only in a reduction of the effective resistance, then within the framework of this calculation the skin depths should be smaller than those calculated. In addition to the electron and ion temperatures, the variables of the problem are the percentage of ionization, the resistivity of the gas, and the current density. Since the current and resistivity are interdependent, the plasma equations are coupled to the field equations.

At the boundary of the plasma the electric field is set equal to a constant applied electric field minus a self-induced electric field. It is also assumed that the current density and its derivative go to zero at large distances from the plasma boundary. Some physical situations for which this model is applicable are discussed along with the results.

II. FIELD EQUATIONS

The problem considered (see Fig. 1) is one dimensional, i.e., the electric field $\underline{E}$, the magnetic field $\underline{H}$, and the current density $\underline{j}$ are functions of y and t. The x component of the magnetic field, $H_x(y,t)$, is the self-magnetic field that results from the current density $j_z(y,t)$; the z component of the magnetic field, H_z, is the externally applied constant stabilizing field. The field equations then are

$$\frac{\partial E_z}{\partial y} = -\frac{1}{c}\frac{\partial B_x}{\partial t}, \quad a \leq y < \infty, \tag{1}$$

$$\frac{\partial H_x}{\partial y} = -\frac{4\pi}{c} j_z , \quad a \leq y < \infty , \tag{2}$$

$$E_z = \eta_z j_z , \quad a \leq y < \infty , \tag{3}$$

where $\eta_z(y,t)$ is the resistivity of the plasma.

Differentiating Eq. (3) with respect to y gives (let $j = j_z$ and $\eta = \eta_z$)

$$\frac{\partial E_z}{\partial y} = \frac{\partial}{\partial y} (\eta j) .$$

Then from Eq. (1)

$$-\frac{1}{c} \frac{\partial B_x}{\partial t} = \frac{\partial}{\partial y} (\eta j) .$$

Now differentiating the above yields

$$-\frac{1}{c} \frac{\partial^2 B_x}{\partial y \, \partial t} = \frac{\partial^2}{\partial y^2} (\eta j) .$$

Differentiating Eq. (2) with respect to t gives

$$\frac{\partial^2 H_x}{\partial t \, \partial y} = -\frac{4\pi}{c} \frac{\partial j}{\partial t} .$$

Using $B_x = \mu H_x$ then gives

$$\frac{\partial j}{\partial t} = \frac{c^2}{4\pi\mu} \frac{\partial^2}{\partial y^2} (\eta j) \tag{4}$$

for $a \leq y < \infty$, $t \geq 0$.

Equation (4) is the differential equation to be solved for the current density $j(y,t)$. It is a nonlinear equation since η depends on j through the plasma equations.

The boundary conditions that are used for Eq. (4) are

$$j \to 0 \text{ as } y \to \infty , \tag{5}$$

and

$$E_e - L \frac{di}{dt} = \eta(a,t) \, j(a,t) , \tag{6}$$

where E_0 is a constant applied electric field,

L is a constant inductance,

and i is the total current, i.e.,

$$i = \int_a^\infty j \, dy. \tag{7}$$

Equation (6) may be rewritten as

$$E_0 - L \frac{d}{dt} \int_a^\infty j \, dy = \eta(a,t) \, j(a,t) ,$$

or

$$E_0 - L \int_a^\infty \frac{\partial j}{\partial t} \, dy = \eta(a,t) \, j(a,t) .$$

Substituting Eq. (4) into the above equation

$$E_0 - \frac{Lc^2}{4\pi\mu} \int_a^\infty \frac{\partial^2}{\partial y^2} (\eta j) \, dy = \eta(a,t) \, j(a,t) ,$$

or

$$E_0 + \frac{Lc^2}{4\pi\mu} \left. \frac{\partial(\eta j)}{\partial y} \right|_{y=a} = \eta(a,t) \, j(a,t) ,$$

where

$$\frac{\partial(\eta j)}{\partial y} \to 0 \quad \text{as} \quad y \to \infty .$$

Let

$$a = \frac{Lc^2}{4\pi\mu} , \tag{8}$$

then the boundary condition becomes

$$E_0 = \eta(a,t) \, j(a,t) - a \left. \frac{\partial(\eta j)}{\partial y} \right|_{y=a} . \tag{9}$$

As an initial condition the resistivity of the gas is taken to be uniform, i.e., $\eta(y,0) = \eta(0)$. The initial current density may then be taken as zero, or an initial current density may be chosen which satisfies the conditions as $y \to \infty$; e.g.,

$$j(y,0) = j_0 e^{-(y-a)/\delta} \tag{10}$$

and to be consistent with the boundary condition Eq. (8) we have

$$j_0 = \frac{E_0}{\eta(0)} \frac{1}{1 + \frac{a}{\delta}} \tag{11}$$

III. PLASMA EQUATIONS

The energy balance equation is

$$\eta j^2 = \alpha \epsilon_0 \frac{\partial n_e}{\partial t} + \frac{\partial}{\partial t} \left(\frac{3}{2} n_e \theta_e + \frac{3}{2} n_i \theta_i \right) , \tag{12}$$

where $\eta(y,t)$ is the resistivity of the plasma,

$j(y,t)$ is the current density,

ϵ_0 is an average ionization potential (16.2 ev),

$\alpha\epsilon_0$ is the average energy expended per ion pair (ion plus electron),

$n_e(y,t) = n_i(y,t)$, the electron and ion densities,

$\theta_e(y,t) = kT_e$, the electron temperature, and

$\theta_i(y,t) = kT_i$, the ion temperature.

The left hand side of Eq. (12) is the rate of ohmic heating per unit volume. It is assumed that this energy goes into the ionization of neutrals and heating of the charged particles. The first term on the right hand side of Eq. (12) is the energy expended on ionization. It essentially represents an energy drain on the electrons. Now the ionization of the deuterium molecule may proceed in various ways and in general is not a one-step process. However, this complexity is avoided by treating the deuterium gas as monatomic with an average ionization potential ϵ_0. The cross section for ionization is taken to be the same as for the ionization of D_2.

Energy losses, such as inelastic collisions of electrons with neutrals, are included in the factor α. For example, if on the average α' excitation collisions occur for each ionization collision with the same dissipation of energy, then the rate of this energy loss per unit volume is $\alpha'\epsilon_0(\partial n_e/\partial t)$. We choose $\alpha = 2$.

Because of the mobility of the electrons, their temperature increases much faster under the influence of the electric field than do the ions. For electric fields of the magnitude employed in pinches, the electrons will rapidly reach a kinetic temperature corresponding to the ionization potential. Because of the mass difference, the electrons give up little energy to the neutrals during their lifetime, i.e., the ionization time is short as compared to an energy-exchange time. It is for this reason that the change in temperature of the neutrals is not included in Eq. (12). At the completion of ionization the electrons lose energy primarily by transferring it to the ions. It is assumed that the bremsstrahlung radiation is negligible for the electron temperatures achieved during the time before the implosion. Charge-exchange effects should also be small for the times of interest at the densities and energies of this problem.

The resistivity of the partially ionized plasma is

$$\eta = \frac{m}{n_e e^2} (\nu_i + \nu_n), \tag{13}$$

where m is the electron mass,

e is the electron charge,

ν_i is the collision frequency of electrons with ions, and

ν_n is the collision frequency of electrons with neutrals.

Electron collisions with neutrals are retained in the definition of electrical resistivity, since the collisions impede the motion of the electrons in the direction of the electric field.

The effective ν_i is

$$\nu_i = \left[\frac{\pi^{3/2}}{4 \times 0.582} \frac{e^4}{(2m)^{1/2}} \ln\left(\frac{b_{max}}{b_{min}}\right) \right] \frac{n_i}{\theta_e^{3/2}} , \qquad (14)$$

where the factor 0.582 accounts for electron-electron collisions,[2] and

$$\nu_n = (n_0 - n_e)(3\theta_e/m)^{1/2} \sigma , \qquad (15)$$

where n_0 = gas density,

and σ = cross section for electron collisions with neutrals.

We take $\sigma = 3 \times 10^{-16}$ cm^2. Note that the resistivity as defined does not depend on the ion density n_i, or on the temperature θ_i, but only on the electron temperature and the fraction of ionization. The neutral particles are treated as stationary targets (i.e., zero temperature).

The ionization equation is

$$\frac{\partial n_e}{\partial t} = n_e(n_0 - n_e) \overline{\sigma_i v_e} , \qquad (16)$$

where σ_i is the ionization cross section, and v_e is the electron velocity.

The ionization cross section is obtained by fitting published experimental results.[3]

$$\begin{aligned}
\sigma_i &= 0, \quad \epsilon < \epsilon_0 = 16.2 \ (1.6 \times 10^{-12}) \text{ ergs} \\
\sigma_i &= 1.20 - \frac{4}{30}\left(\frac{\epsilon}{\epsilon_0} - 4\right)^2, \quad \epsilon_0 < \epsilon < 4\epsilon_0 \\
\sigma_i &= 1.36 - 0.04 \frac{\epsilon}{\epsilon_0}, \quad 4\epsilon_0 < \epsilon < 20\epsilon_0 \\
\sigma_i &= 0.56, \quad \epsilon > 20\epsilon_0 ,
\end{aligned} \qquad (17)$$

where σ_i is expressed in units of πa_0^2.

---

[2] See Lyman Spitzer, Jr., Physics of Fully Ionized Gases (Interscience Publishers, Inc., New York, 1956), p. 84.

[3] E.g., N.F. Mott and H.S.W. Massey, The Theory of Atomic Collisions (Clarendon Press, Oxford, 1949), second edition, p. 245.

The quantity $\overline{\sigma_i v_e}$ is obtained by averaging over a Maxwell-Boltzmann distribution. Then

$$\overline{\sigma_i v_e} = -2a_0^2 \left(2\pi \frac{\theta_e}{m}\right)^{1/2} \left[\left(-0.8 - \frac{4}{3}\frac{1}{a} + 0.8\frac{1}{a^2}\right) e^{-a} + \left(0.16 - 0.987\frac{1}{a} - 0.8\frac{1}{a^2}\right) e^{-4a} + \left(-0.8 - 0.08\frac{1}{a}\right) e^{-20a}\right], \quad (18)$$

where $a = \epsilon_0/\theta_e$.

The equation giving the rate at which energy is transferred from electrons to ions is

$$\frac{\partial \theta_i}{\partial t} = \frac{8}{3}(2\pi)^{1/2} e^4 n_e \frac{m^{1/2}}{M} \frac{\theta_e - \theta_i}{\theta_e^{3/2}} \ln\left(\frac{b_{max}}{b_{min}}\right), \quad (19)$$

where M is the ion mass.

IV. SUMMARY AND METHOD OF SOLUTION

Let $f = n_e/n_0 = n_i/n_0$, and let θ_e, θ_i be expressed in units of ϵ_0, the ionization potential. Let η be in units of $\eta_0 = 4\pi\mu/c^2$, then we can summarize the equations to be solved:

$$\frac{\partial j}{\partial t} = \frac{\partial^2(\eta j)}{\partial y^2} \quad (20)$$

$$A_6 E_0 = \eta(a,t)\, j(z,t) - a \left.\frac{\partial(\eta j)}{\partial y}\right|_{y=a} \quad (21)$$

$$\eta = A_2\left(\frac{1}{f} - 1\right)\theta_e^{1/2} + A_3\theta_e^{-3/2} \quad (22)$$

$$\frac{\partial \theta_e}{\partial t} = -\frac{\partial \theta_i}{\partial t} - \left(\frac{2a}{3} + \theta_e + \theta_i\right)\frac{1}{f}\frac{\partial f}{\partial t} + A_1 \frac{1}{f}\eta j^2 \quad (23)$$

$$\frac{\partial \theta_i}{\partial t} = A_5 f \theta_e^{-3/2} (\theta_e - \theta_i) \tag{24}$$

$$\frac{\partial f}{\partial t} = A_4 f(1-f)\theta_e^{1/2}\left(0.8 + \frac{4}{3}\theta_e - 0.8\theta_e^2\right)e^{-1/\theta_e} + \left(-0.16 + 0.987\theta_e + 0.8\theta_e^2\right)e^{-4/\theta_e} + (0.8 + 0.08\theta_e)e^{-20/\theta_e}, \tag{25}$$

where the constants are

$$A_1 = \frac{2}{3}\frac{\eta_0}{n_0 \epsilon_0}$$

$$A_2 = \frac{\sigma}{\eta_0 e^2}(3m\epsilon_0)^{1/2}$$

$$A_3 = \left(\frac{\pi}{2\epsilon_0}\right)^{3/2} m^{1/2} \frac{e^2}{2 \times 0.582\, \eta_0} \ln \frac{b_{max}}{b_{min}}$$

$$A_4 = 2a_0^2 n_0 (2\pi\epsilon_0/m)^{1/2}$$

$$A_5 = \frac{8}{3}\frac{(2\pi m)^{1/2}}{M} n_0 e^4 \epsilon_0^{-3/2} \ln \frac{b_{max}}{b_{min}}$$

$$A_6 = \frac{1}{\eta}.$$

The solutions of Eqs. (22)-(25) with j = constant is the problem considered in the paper of Wyld and Watson.[1] The resulting set of ordinary differential equations can be solved numerically.

If we let η = constant, Eq. (20) becomes

$$\frac{\partial j}{\partial t} = \eta \frac{\partial^2 j}{\partial y^2}, \quad a \leq y < \infty, \quad t \geq 0;$$

with boundary conditions

$$j(a,t) - a \left.\frac{\partial j}{\partial y}\right|_{y=a} = \frac{E_0}{\eta}$$

$$j(y,t) \to 0 \quad \text{as} \quad y \to \infty$$

and initial condition

$$j(y,0) = j_0 e^{-[(y-a)/\delta]}$$

where

$$j_0\left(1 + \frac{a}{\delta}\right) = \frac{E_0}{\eta} \ .$$

This problem can be solved by using the Laplace transformation and the solution is

$$j(y,t) = \frac{E_0}{\eta}\left[1 - \frac{\eta}{\delta^2}\,\frac{\eta^{1/2}}{a}\,\frac{2}{\pi}\int_0^\infty \frac{e^{-tx^2}\left[\frac{\eta^{1/2}}{a}\sin\frac{y-a}{\eta^{1/2}}x + x\cos\frac{y-a}{\eta^{1/2}}x\right]dx}{x\left(x^2 + \frac{\eta}{\delta^2}\right)\left(x^2 + \frac{\eta}{a^2}\right)}\right] .$$

The above solution to this special case can be evaluated in terms of error functions and is quite useful in checking the results in the early stages of the more general calculation. In order to solve the complete system of equations (20)-(25), we solve a set of finite difference equations. Consider the mesh (Fig. 2), where $a = \ell_0 \Delta y$. The implicit difference equation corresponding to (20) is

$$j_\ell^{n+1} - j_\ell^n = \frac{\Delta t}{2(\Delta y)^2}\left(\eta_{\ell+1}^{n+1}\, j_{\ell+1}^{n+1} - 2\eta_\ell^{n+1}\, j_\ell^{n+1} + \eta_{\ell-1}^{n+1}\, j_{\ell-1}^{n+1}\right)$$

$$+ \frac{\Delta t}{2(\Delta y)^2}\left(\eta_{\ell+1}^{n}\, j_{\ell+1}^{n} - 2\eta_\ell^{n}\, j_\ell^{n} + \eta_{\ell-1}^{n}\, j_{\ell-1}^{n}\right) ,$$

$$\ell = \ell_0 + 1, \ldots, L-1 .$$

The boundary condition at $y = a$ becomes

$$E_0 = \eta_{\ell_0}{}^{n+1} \; j_{\ell_0}{}^{n+1} - \ell_0 \left(\eta_{\ell_0+1}{}^{n+1} \; j_{\ell_0+1}{}^{n+1} - \eta_{\ell_0}{}^{n+1} \; j_{\ell_0}{}^{n+1} \right) .$$

The maximum value of y in the mesh is $L\Delta y$. In order to treat the imposed conditions on j as $y \to \infty$, j_L is set equal to zero, but the distance $L\Delta y$ must be taken large enough so that the solution is not affected by changes in the cut-off. The cut-off distance is a result of numerical experimentation and differs with the various cases presented. The method of solution of the implicit difference equations is given by Richtmyer.[4]

The Eqs. (23)-(25) must be solved at each value of ℓ in the mesh. Since they do not contain spatial derivatives, they can be considered as ordinary differential equations and solved by a standard method for each ℓ.

V. RESULTS AND MODELS

It is known that in addition to an externally applied B_z, a surrounding conducting wall enhances the stability of a plasma column. Suppose in Fig. 1 that the plane at $y = 0$ is a conductor. If the region $0 \leq y \leq a$ is occupied by a dielectric and a plasma occupies the region $y \geq a$, then a charge density is deposited on the surface of the dielectric which neutralizes the polarization charge density, and the electric field lines in the plasma then do not terminate on the surface but run in the z direction as assumed in the model.

We can derive the boundary condition at $y = a$ under these conditions. Integrating Eq. (1) with respect to y gives

$$E_z(y,t) - E_0 = -\frac{a}{c} \frac{\partial}{\partial t} B_x(a,t) - \frac{1}{c} \frac{\partial}{\partial t} \int_a^y B_x(\zeta, t) \, d\zeta .$$

---

[4] R. D. Richtmyer, Difference Methods for Initial-Value Problems (Interscience Publishers, New York, 1957), p. 101.

We must have $E_z(y,t) \to 0$ as $y \to \infty$, so

$$E_0 = \frac{a}{c}\frac{\partial}{\partial t} B_x(a,t) - \frac{1}{c}\frac{\partial}{\partial t}\int_a^\infty B_x(y,t)\, dy . \tag{26}$$

Integration of Eq. (2) gives

$$H_x(y,t) - H_x(a,t) = -\frac{4\pi}{c}\int_a^y j(\zeta,t)\, d\zeta .$$

We must have $H_x(y,t) \to 0$ as $y \to \infty$, so

$$H_x(a,t) = \frac{4\pi}{c}\int_a^\infty j(y,t)\, dy . \tag{27}$$

Hence

$$H_x(y,t) = \frac{4\pi}{c}\int_a^\infty j(y,t)\, dy - \frac{4\pi}{c}\int_a^y j(\zeta,t)\, d\zeta ,$$

or

$$H_x(y,t) = \frac{4\pi}{c}\int_y^\infty j(\zeta,t)\, d\zeta . \tag{28}$$

Using Eqs. (27) and (28) in (26) we have

$$E_0 = \frac{4\pi a\mu}{c^2}\frac{\partial}{\partial t}\int_a^\infty j(\zeta,t)\, d\zeta + \frac{4\pi\mu}{c^2}\frac{\partial}{\partial t}\int_a^\infty dy \int_y^\infty j(\zeta,t)\, d\zeta .$$

Integrating the second term by parts we have

$$E_0 = \frac{4\pi\mu}{c^2}\frac{\partial}{\partial t}\left[a\int_a^\infty j(\zeta,t)\, d\zeta - a\int_a^\infty j(\zeta,t)\, d\zeta + \int_a^\infty y\, j(y,t)\, dy\right]$$

or

$$E_0 = \frac{4\pi\mu}{c^2}\int_a^\infty y\frac{\partial j}{\partial t}\, dy . \tag{29}$$

Now using Eq. (4) in Eq. (29) we have

$$E_0 = \int_a^\infty y\frac{\partial^2(\eta j)}{\partial y^2}\, dy .$$

Integrating by parts we have

$$E_0 = \left[y \frac{\partial(\eta j)}{\partial y} \right]_a^\infty - \int_a^\infty \frac{\partial(\eta j)}{\partial y} \, dy .$$

We have assumed $\eta(y,t)\, j(y,t) \to 0$ as $y \to \infty$,

and if we assume $y \frac{\partial(\eta j)}{\partial y} \to 0$ as $y \to \infty$;

then

$$E_0 = \eta(a,t)\, j(a,t) - a \left. \frac{\partial(\eta j)}{\partial y} \right|_{y=a}$$

is the boundary condition at $y = a$. This corresponds to Eq. (9), where a is now taken to be the thickness of an insulating region between the conducting shell and the plasma. This distance fixes the inductance in Eq. (6) by using Eq. (8).

For an $a = 1$ cm we present two cases of interest. The first case is for an applied electric field $E_0 = 100$ v/cm, and the gas density $n_0 = 10^{15}/\text{cm}^3$. This case corresponds to pinch devices at Livermore and Los Alamos. In Fig. 4 the values of the plasma and field variables at the plasma boundary are plotted as a function of time. In Fig. 5, $j(y,t)$ is plotted as a function of distance from the wall for successive times. In Fig. 6 the plasma variables are plotted as a function of distance from the wall at a time corresponding to completion of ionization at the plasma boundary.

The second case for $a = 1$ cm is for an $E_0 = 2$v/cm and $n_0 = 10^{13}/\text{cm}^3$. This case is intended to correspond to a large pinch device such as Zeta at Harwell. Similar results for this case are presented in Figs. 10-12.

Another physical situation for which the model applies is shown in Fig. 3. Consider a torus with a nonconducting shell, and assume that the minor radius r_0 is small compared to the major radius R, and that the current skin depth δ is small as compared to the minor radius; i.e., $r_0/R \ll 1$; $\delta/r_0 \ll 1$.

Integrating $\nabla \times \underline{H} = \frac{4\pi}{c} \underline{j}$ over the area enclosed by the curve ABCD, which is within the current layer, gives

$$\oint \underline{H} \cdot d\underline{s} = \frac{4\pi}{c} \int_0^{r_0} 2\pi r j \, dr$$

or, using the above assumption,

$$2\pi r_0 H_\theta = \frac{4\pi}{c} \, 2\pi r_0 \int_0^{r_0} j \, dr .$$

Suppose the field in the symmetry plane containing the torus is obtained by treating the torus as a single circular current loop. This field may be approximated by the analytic expression

$$H_\theta = \frac{i}{c} \left(\frac{2}{r} + \frac{4}{R} \right) .$$

The total flux due to the plasma current that passes through the symmetry plane and enclosed by the torus is

$$\phi = 2\pi\mu \int_R^{r_0} H_\theta \, (R - r) \, dr ,$$

and using the above expression for H_θ gives

$$\phi = 4\pi\mu R \, \frac{i}{c} \, (a^2 - a - \ln a) ,$$

where $a = r_0/R$.

Using the analytic expression for H_θ gives a total enclosed flux that agrees to within $\frac{1}{2}\%$ of the numerical result. Now in the center of the torus, i.e., at $r = R$, assume that there is a changing externally applied magnetic field that gives a constant electric field E_0 at the plasma.

$$E_0 = - \frac{1}{c} \, \frac{1}{2\pi R} \, \frac{\partial \phi_0}{\partial t}$$

Hence the electric field at the boundary of the plasma is

$$E_B = E_0 - \frac{2\mu}{c^2} \, (a^2 - a - \ln a) \, \frac{\partial i}{\partial t} .$$

In our one-dimensional model we have from Eqs. (6) and (8)

$$E_B = E_0 - \frac{4\pi\mu}{c^2} a \frac{\partial i'}{\partial t} ,$$

where $i' = i/2\pi r_0$ for the torus, so

$$a/r_0 = a^2 - a - \ln a . \qquad (30)$$

Equation (30) enables us to calculate an effective value of a in our one-dimensional model for a particular torus.

Consider a small torus where $r_0 = 5$ cm and r_0/R is about $\frac{1}{8}$, then a/r_0 is about 2. For the case $a = 10$ cm, we present a case with $E_0 = 100$ v/cm and $n_0 = 10^{15}/cm^3$ in Figs. 7-9.

Now consider a large torus where $r_0 = 50$ cm and $R = 160$ cm, then a/r_0 is about 1. For the case $a = 50$ cm, we present a case with $E_0 = 2$ v/cm and $n_0 = 10^{13}/cm^3$ in Figs. 13-15.

Three additional cases are presented to show the dependence of boundary-layer formation on density for a large torus. We consider a device with $E_0 = 1$/cm and $a = 10$ cm. The densities taken are $10^{13}/cm^3$, $10^{14}/cm^3$, and $10^{15}/cm^3$. These results are presented in Figs. 16-19.

VI. DISCUSSION OF RESULTS

In order to justify the assumption that magnetohydrodynamic motion, thermal conduction, and particle diffusion can be neglected, the strength of the axial field, H_z, must be stated for each case considered. In present experiments $H_z^2/8\pi$ is approximately equal to $200\epsilon_0 n_0$, where ϵ_0 is the ionization potential and n_0 the gas density. The validity of the assumptions will be compared on this basis.

In Table I is shown the value of the applied H_z appropriate for each case and the ratio, H_x/H_z, of the computed self-field H_x, at the wall, at

Table I. Comparison of the values of plasma variables at the boundary at a time when the ionization is complete at the boundary.

Case	Time in μsec	H_z gauss	$\frac{H_x}{H_z}$	$\frac{H_x^2/8\pi}{n_e\left(\frac{3}{2}\theta_e+\frac{3}{2}\theta_i+2\epsilon_0\right)}$	$\frac{\partial q_T}{\partial y}\Big/ nj^2$	$\frac{\partial q_p}{\partial y}\Big/\frac{\partial n_e}{\partial t}$
$E_0 = 100$ v/cm $n_0 = 10^{15}/cm^3$ $a = 10$ cm	1.00	10^4	0.1	0.5	2.0×10^{-4}	3.5×10^{-3}
$E_0 = 100$ $n_0 = 10^{15}$ $a = 1$	0.25	10^4	0.3	0.6	4.3×10^{-5}	7.0×10^{-3}
$E_0 = 2$ $n_0 = 10^{13}$ $a = 50$	40.0	10^3	0.2	0.4	8.2×10^{-5}	4.1×10^{-2}
$E_0 = 2$ $n_0 = 10^{13}$ $a = 1$	10.0	10^3	1.1	1.5	2.2×10^{-3}	7.4×10^{-3}

a time when ionization at the wall is essentially complete, to the constant field H_z. In addition the ratio of the energy density of the self-field, $H_x^2/8\pi$, to the energy density of the plasma, $\frac{3}{2} n_e\theta_e + \frac{3}{2} n_i\theta_i + 2n_0\epsilon_0$ is listed for the same time. These ratios are calculated at the plasma boundary.

In the energy balance equation, (12), the thermal conduction term, $\partial q_T/\partial y$, is neglected, where

$$q_T = -\frac{5}{2}\frac{n_e\theta_e}{m}\frac{\tau}{1+\omega^2\tau^2}\frac{\partial\theta_e}{\partial y}.$$

In this expression

$$\frac{1}{\tau} = \nu_i + \nu_n = \frac{n_e e^2}{m}\,\eta ,$$

$$\omega = \frac{eH_z}{mc} .$$

In Table I, $\partial q_T/\partial y$ is compared to ηj^2, at the wall. It appears that the assumption is valid.

In the ionization equation, (16), the particle diffusion term, $\partial q_p/\partial y$, is neglected, where

$$q_p = \frac{\theta_e}{m}\,\frac{\tau}{1+\omega^2\tau^2}\,\frac{\partial n_e}{\partial y} .$$

In Table I, $\partial q_p/\partial y$ is compared to $\partial n_e/\partial t$, at the wall. It appears that neglecting this term is a reasonable assumption.

We may examine the numerical results presented to learn the dependence of boundary-layer formation on the parameters varied. These parameters are E_0, n_0, and the inductive term, a. The initial values of the dependent variables were not varied in these cases. In the cases presented the initial values were $j(y,0) = 0$; $\theta_e(y,0) = 1$ ev; $q_1(y,0) = 0$; $f = 0.01$. The effect of changing these initial conditions has also been studied numerically, but those results are not presented in this paper. If instead of $j(y,0) = 0$, we take an initial distribution according to Eq. (10), the current distribution at later times becomes essentially equivalent to the case for $j(y,0) = 0$. This property is characteristic of this type of differential equation. If we vary the initial ionization, the time scale for complete ionization is changed accordingly, but the boundary-layer formation proceeds in the same manner.

In the first two cases (E_0 = 100 v/cm, $n_0 = 10^{15}/cm^3$) and the second two cases (E_0 = 2, $n_0 = 10^{13}$), the effect of changing the inductive term, a, is studied. The effect is quite apparent – the smaller the value of a, the faster and sharper the sheath formation.

In examining these cases it is interesting to note the behavior of the resistivity, η, as a function of electron temperature. In some cases, in the early stages of the ionization phase the resistivity increases with increasing temperature. This can be understood by considering Eq. (22). For low ionization the electron-neutral term dominates. In this early high-resistive phase the current layer broadens considerably. Later, when the gas near the wall becomes more highly ionized, the resistivity drops and a sharp sheath forms.

On going from the small, fast pinches (E_0 = 100, $n_0 = 10^{15}$) to the cases with lower field and density, the differences in time and length scales for boundary-layer formation become apparent. From these results approximate scaling laws can be obtained to predict the results of new cases. For detailed information on current and field distributions, however, the equations need to be solved for new cases.

The last three cases (E_0 = 1, a = 10 cm) have been studied to show the dependence of plasma formation on gas density. The three densities considered are $n_0 = 10^{13}/cm^3$, $n_0 = 10^{14}/cm^3$, $n_0 = 10^{15}/cm^3$. If we consider the ratio of field to pressure, E_0/p, where E_0 is in v/cm and p is in mm of Hg, then these three cases give an E_0/p = 3000, 300, and 30, respectively. From experimental experience we would not expect a sharp boundary-layer formation in the last case. In the first case (E_0/p = 3000) the time for complete ionization at the wall is 25 μsec. The current density

forms a sharp layer. In the second case ($E_0/p = 300$), the time for complete ionization at the wall is 50 μsec. The layer half-width is about ten times the previous case, but a boundary layer has formed. In the third case complete ionization at the wall takes 230 μsec, but the spatial distributions of all the plasma variables indicate that the familiar thin-current sheath has not formed.

The computations were performed on the IBM 704 at Livermore. The programming was done by Mr. Garrett Boer of the Computation Division.

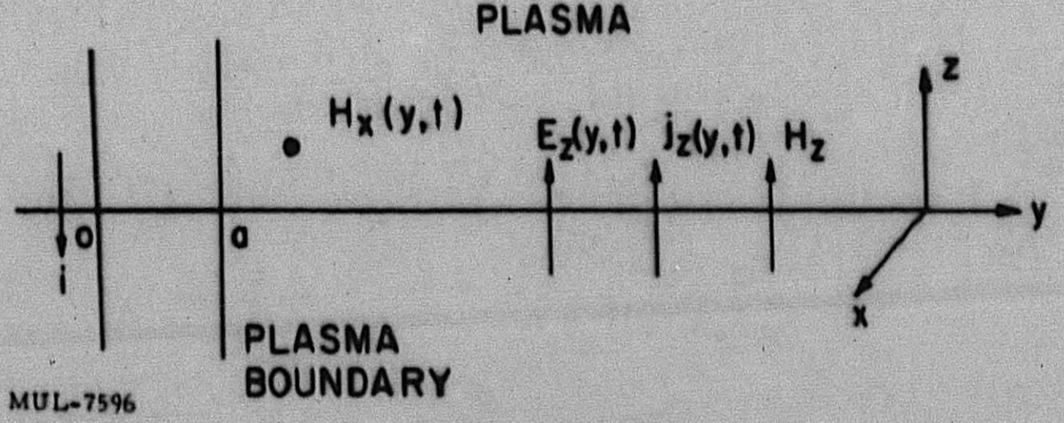

Fig. 1. The field variables.

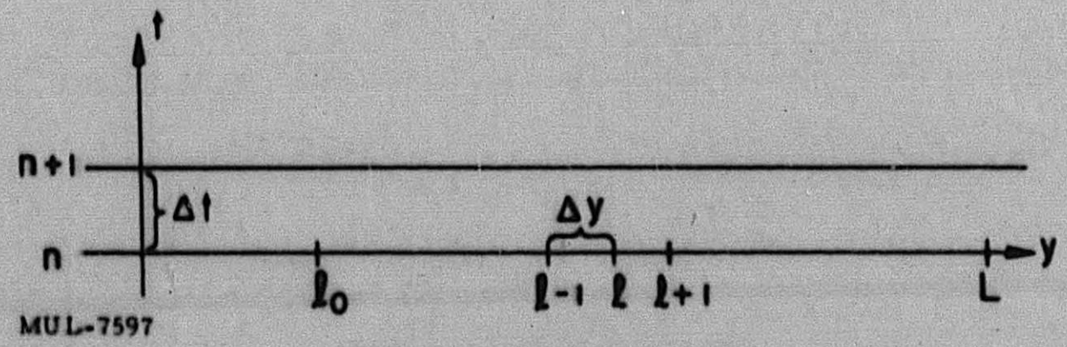

Fig. 2. Difference mesh.

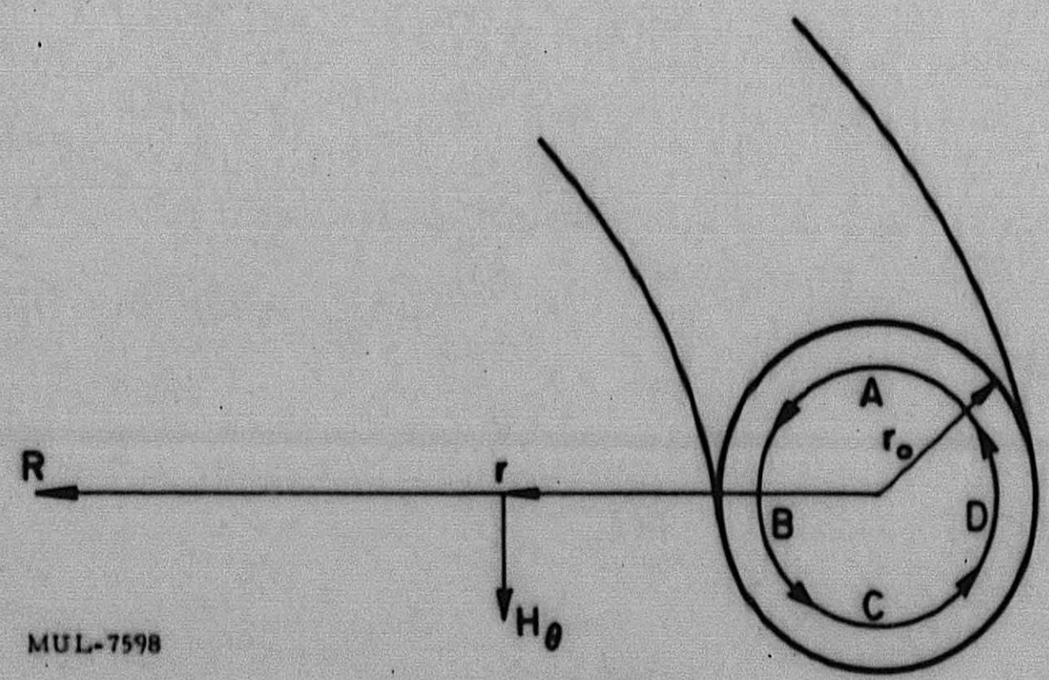

MUL-7598

Fig. 3. Torus model.

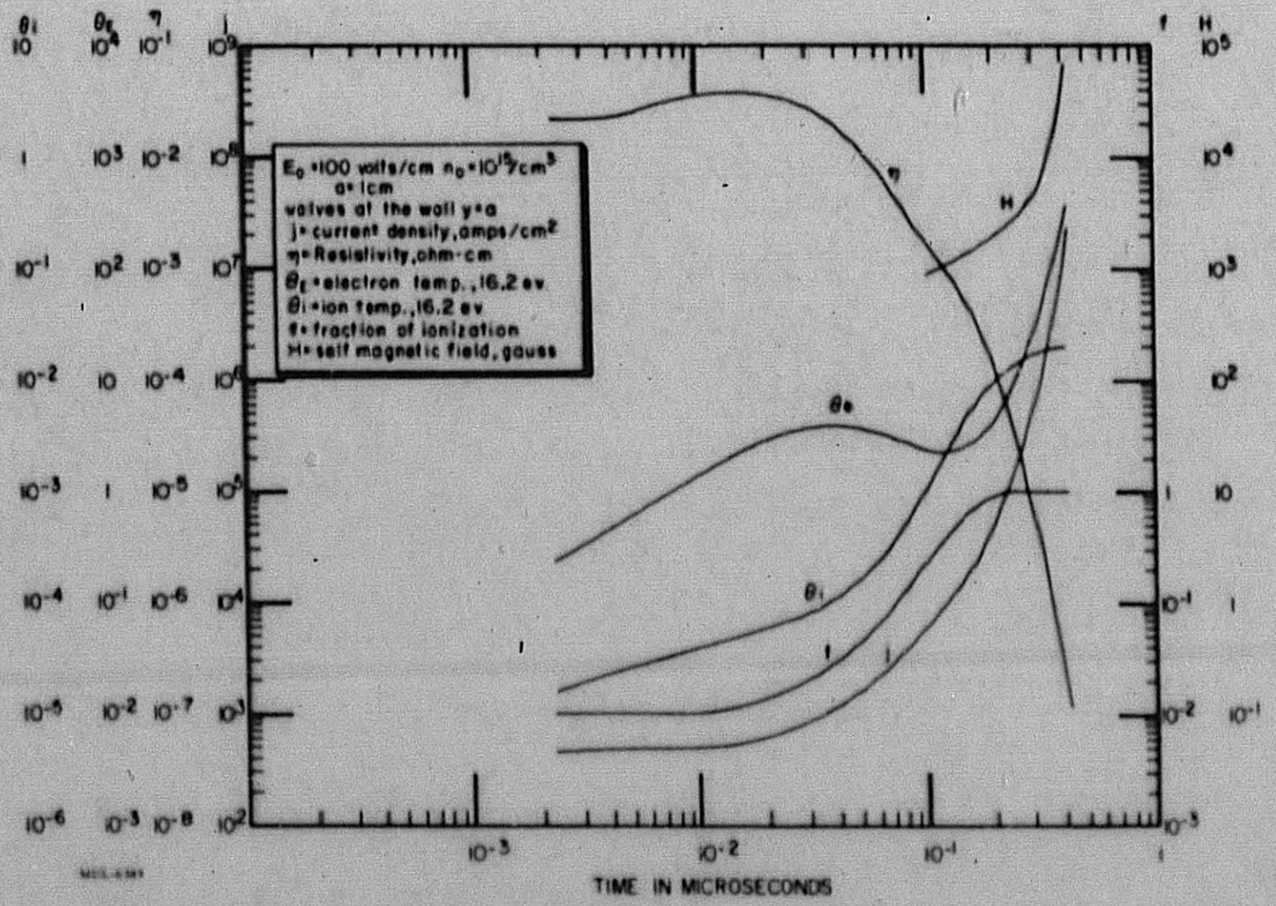

Fig. 4. Time variation of field and plasma variables at the wall.

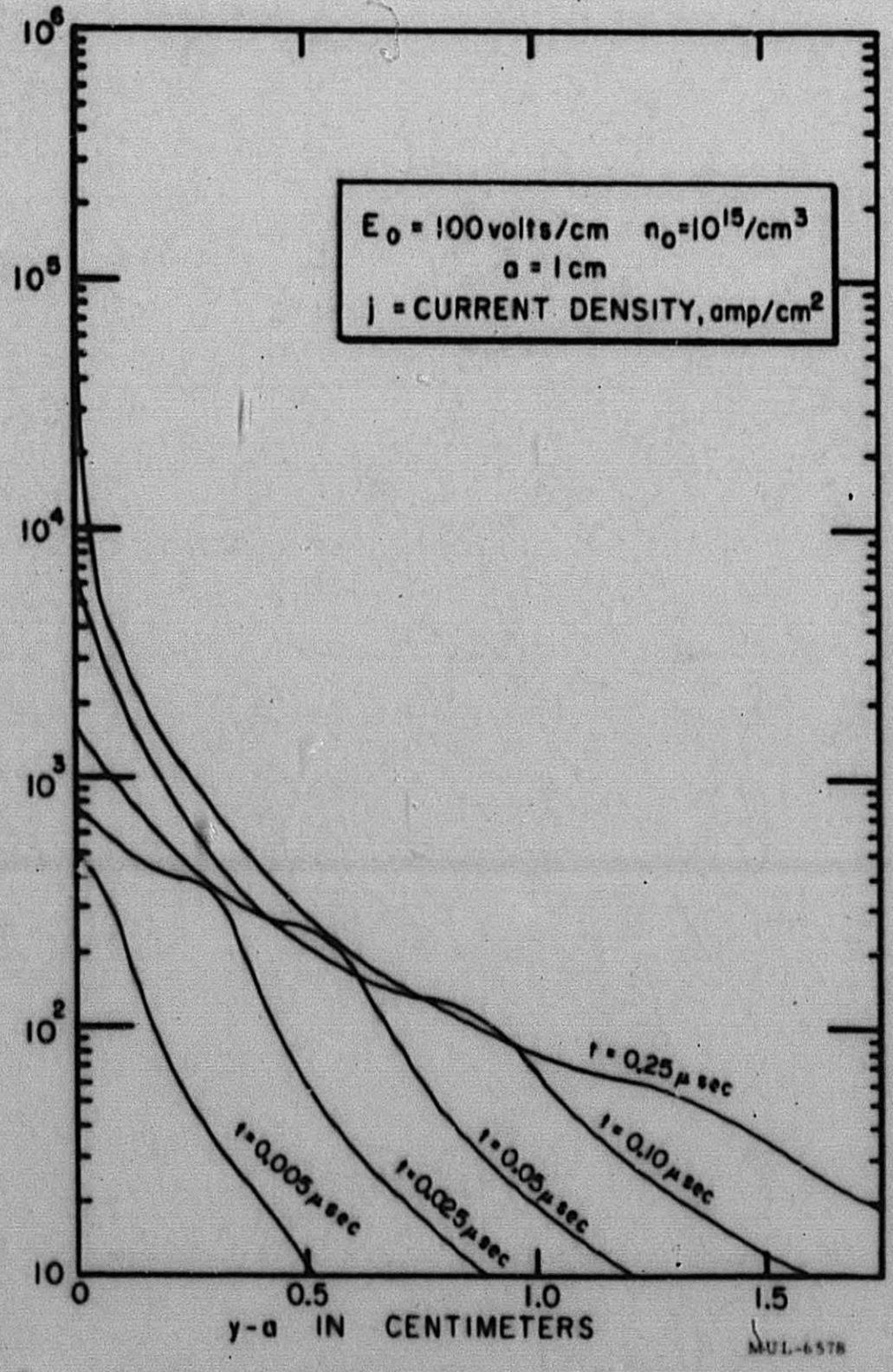

Fig. 5. Current densities at successive times.

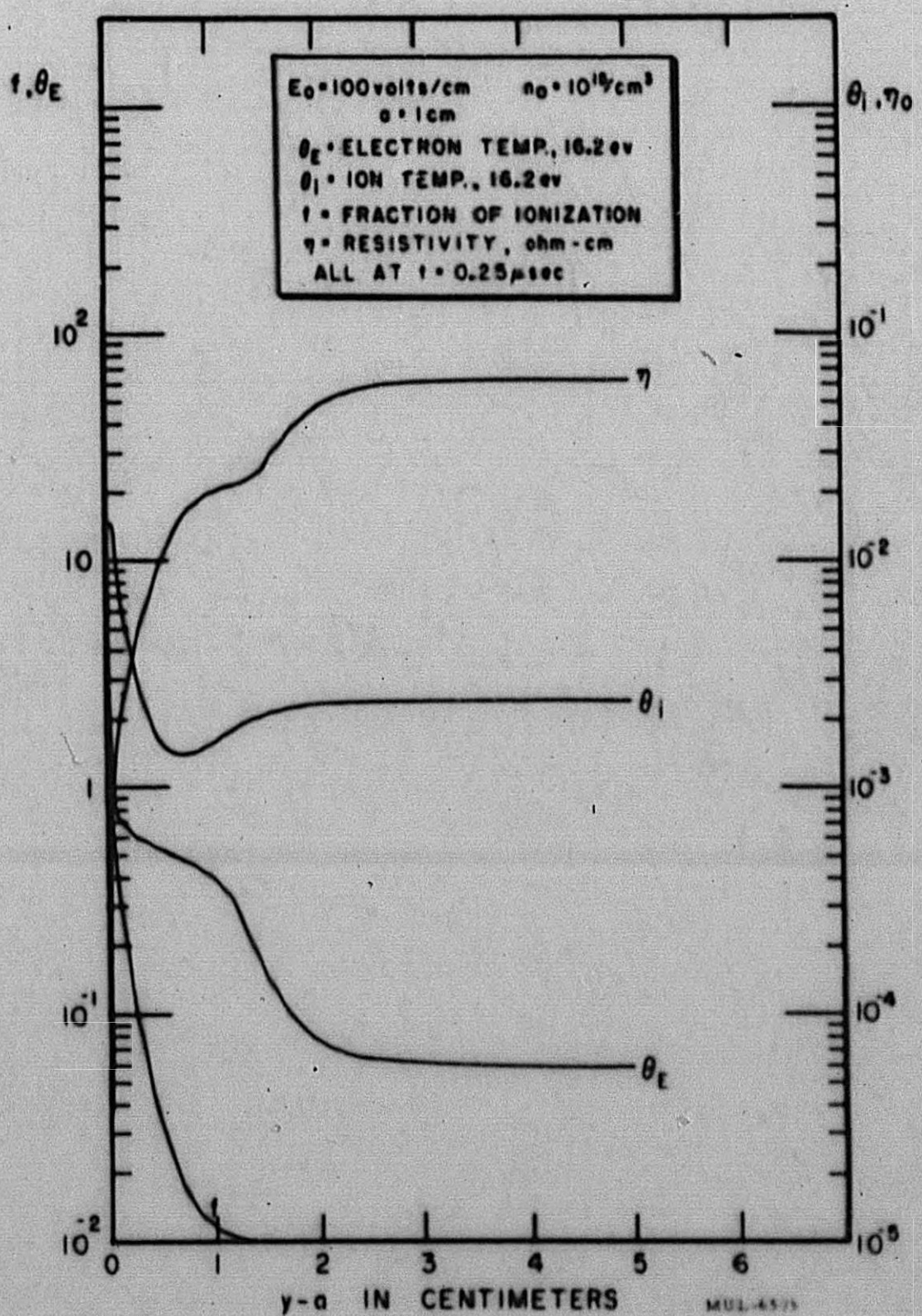

Fig. 6. Spatial distribution of plasma variables.

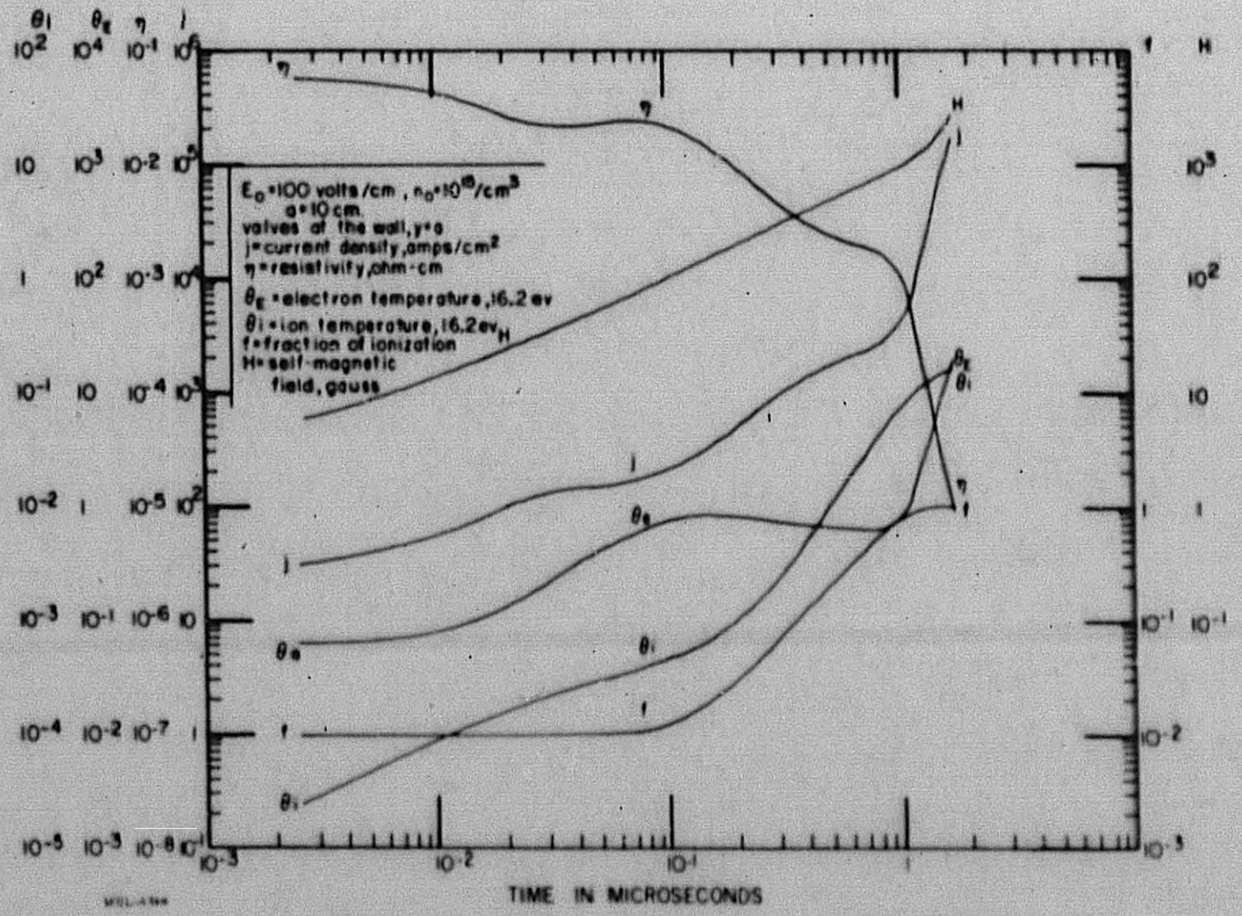

Fig. 7. Time variation of field and plasma variables at the wall.

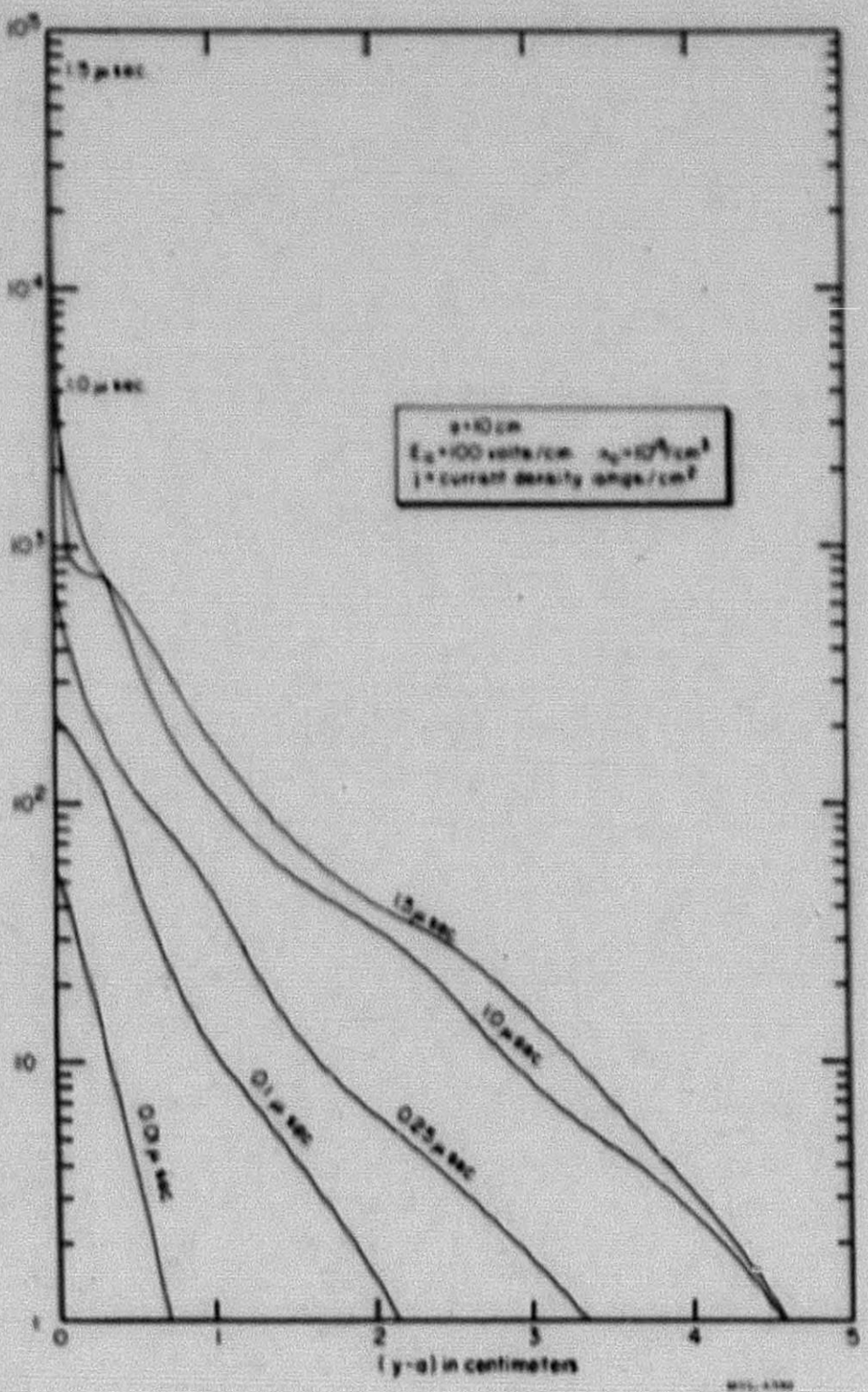

Fig. 8. Current densities at successive times.

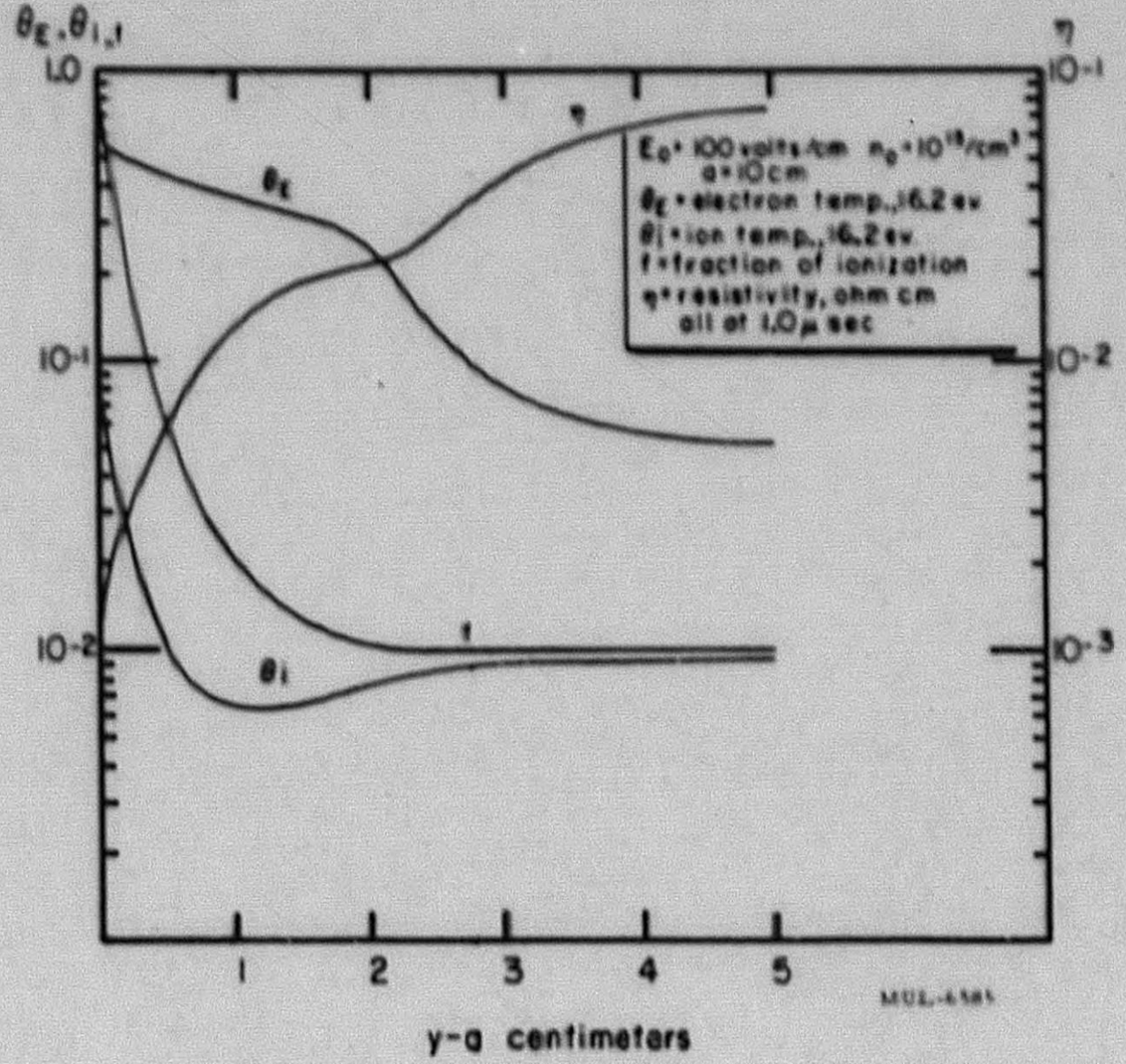

Fig. 9 Spatial distribution of plasma variables.

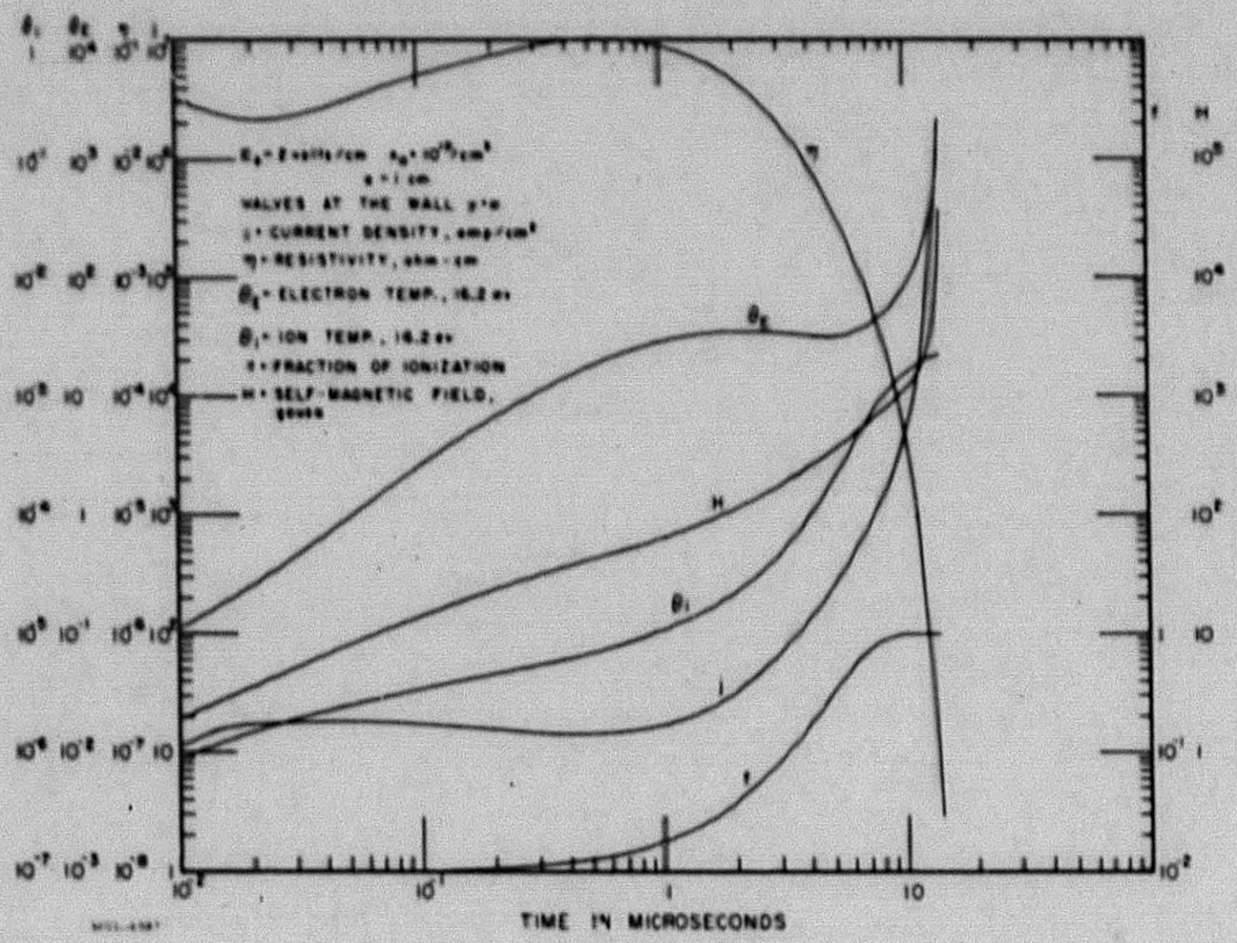

Fig. 10. Time variation of field and plasma variables at the wall.

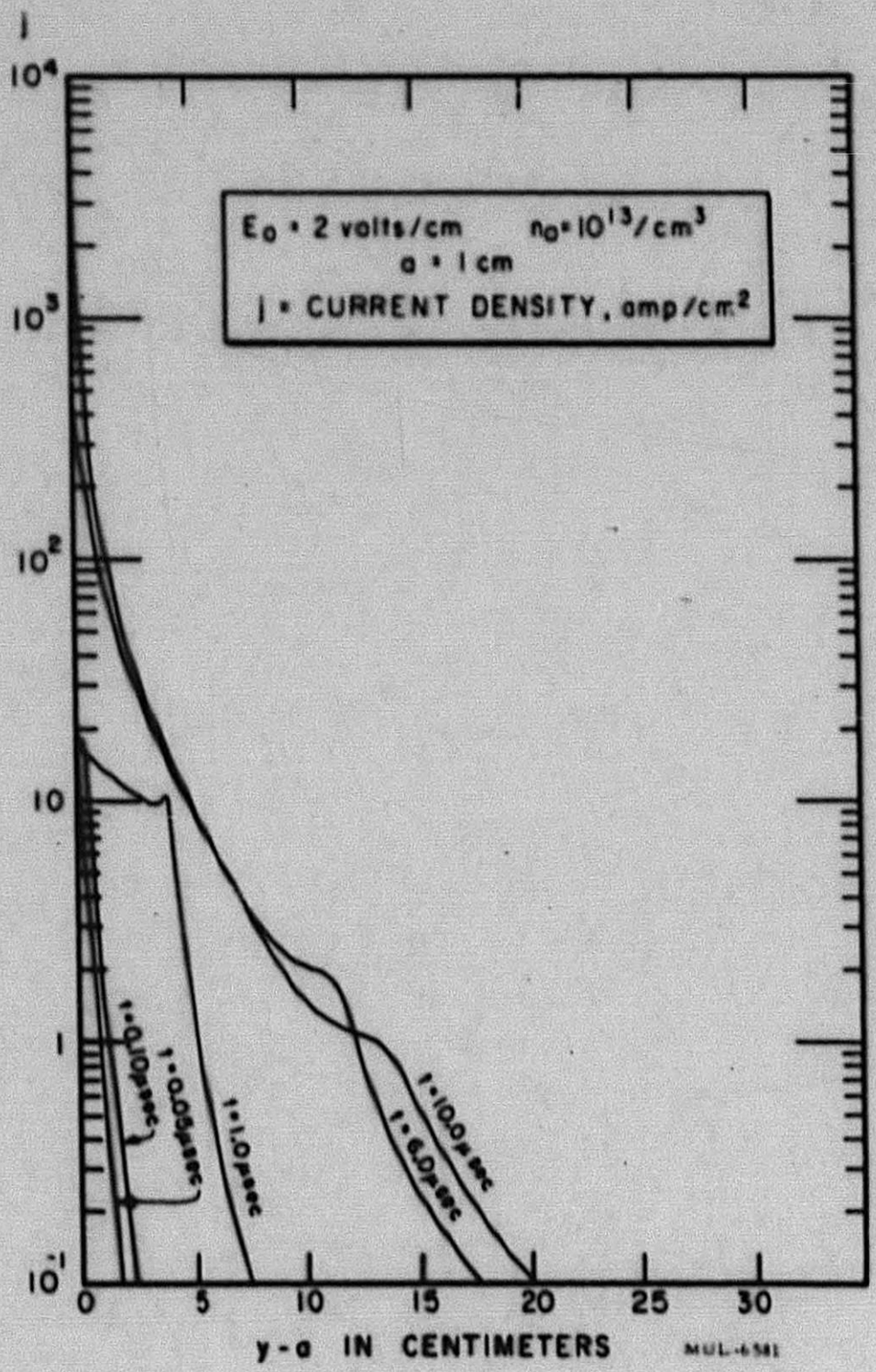

Fig. 11. Current densities at successive times.

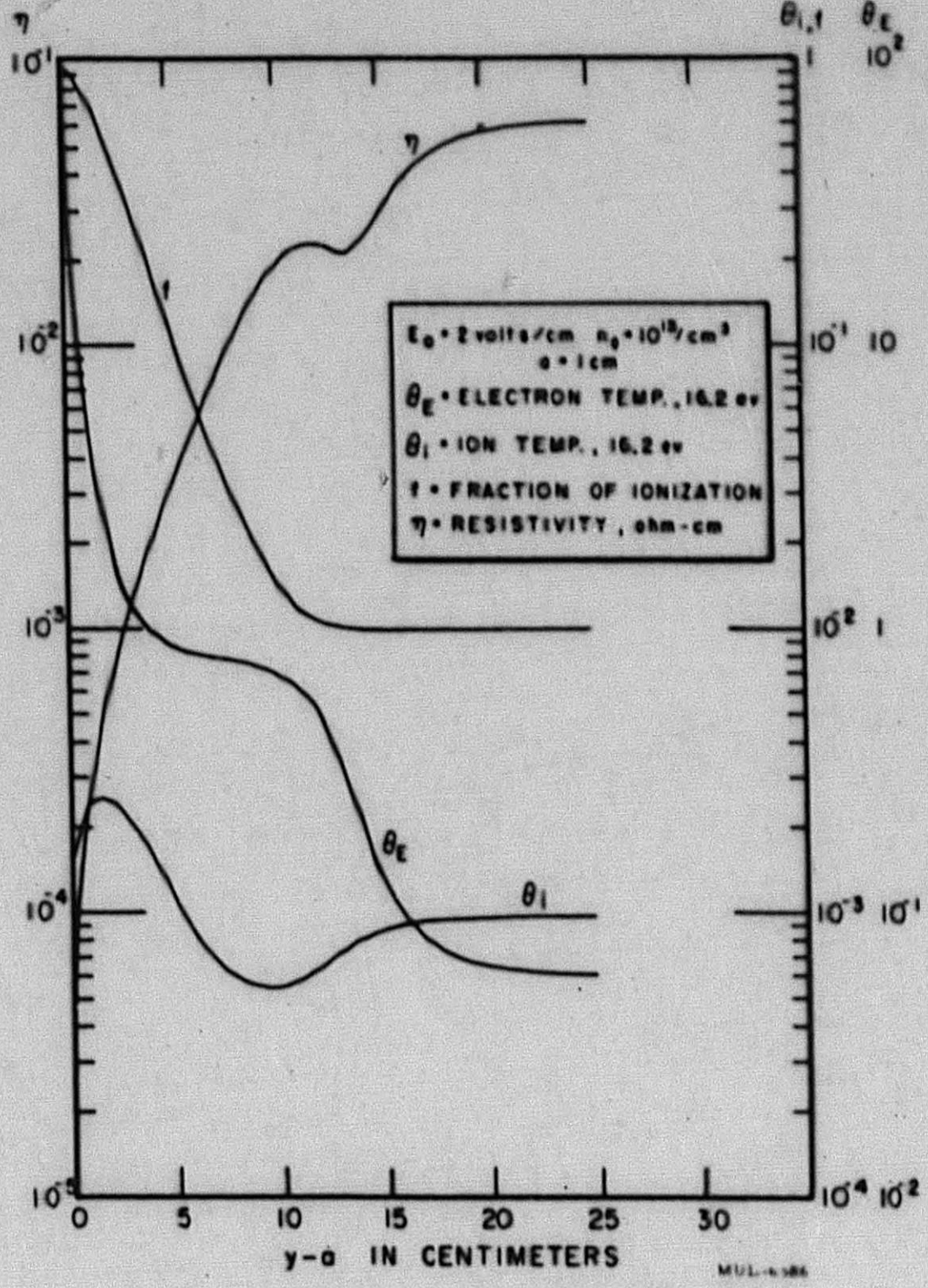

Fig. 12. Spatial distribution of plasma variables.

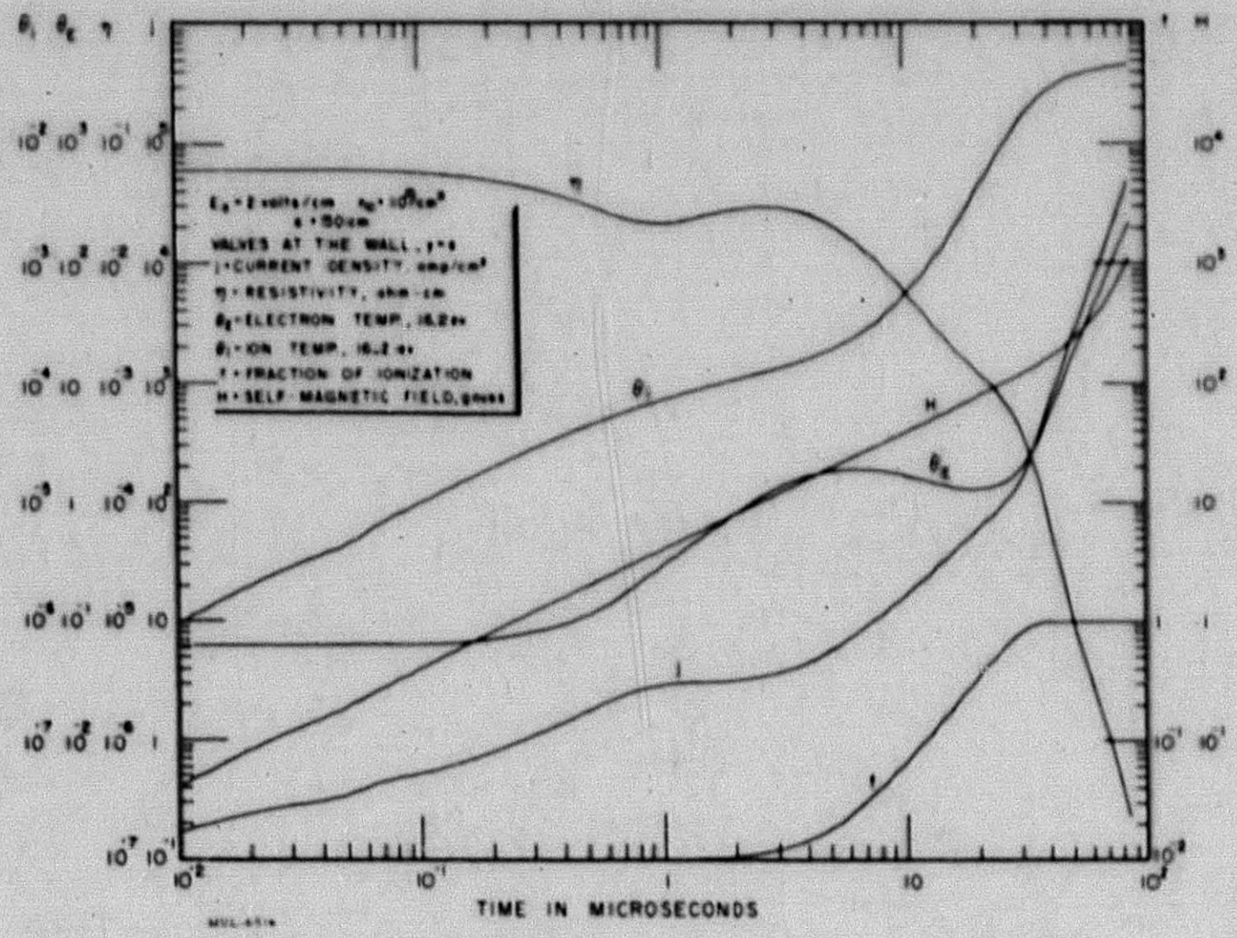

Fig. 13. Time variation of field and plasma variables at the wall.

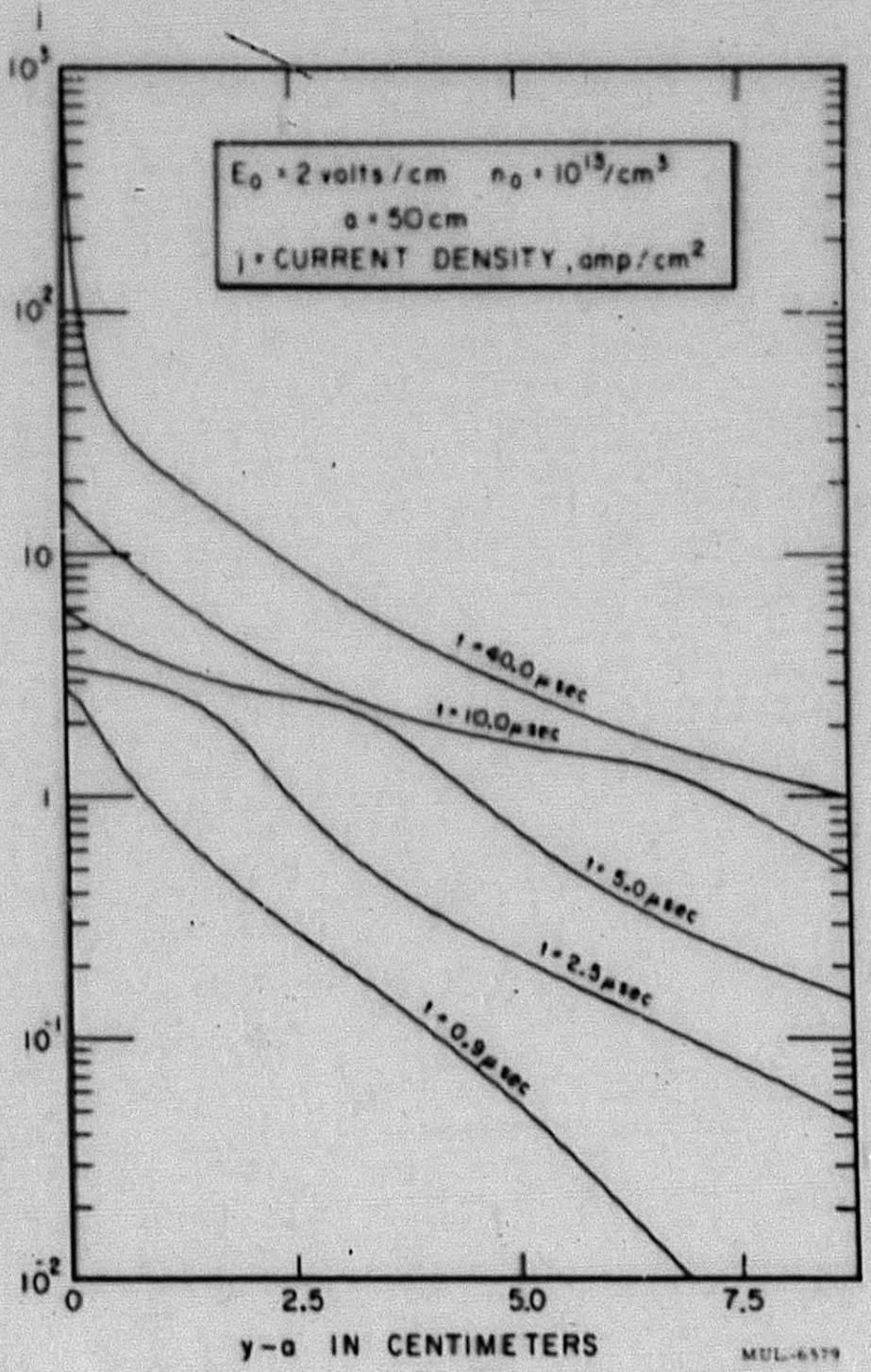

Fig. 14. Current densities at successive times.

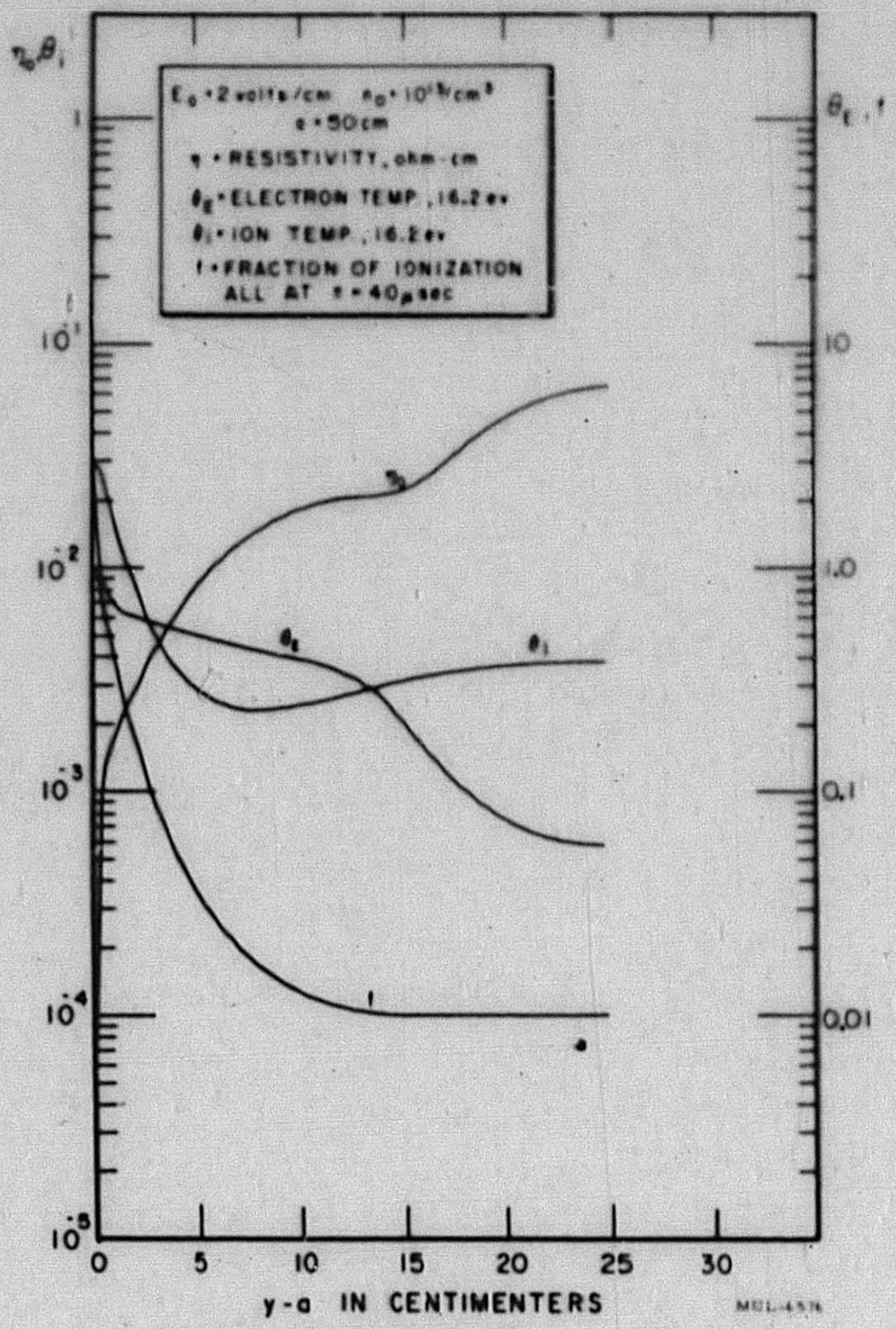

Fig. 15. Spatial distribution of plasma variables.

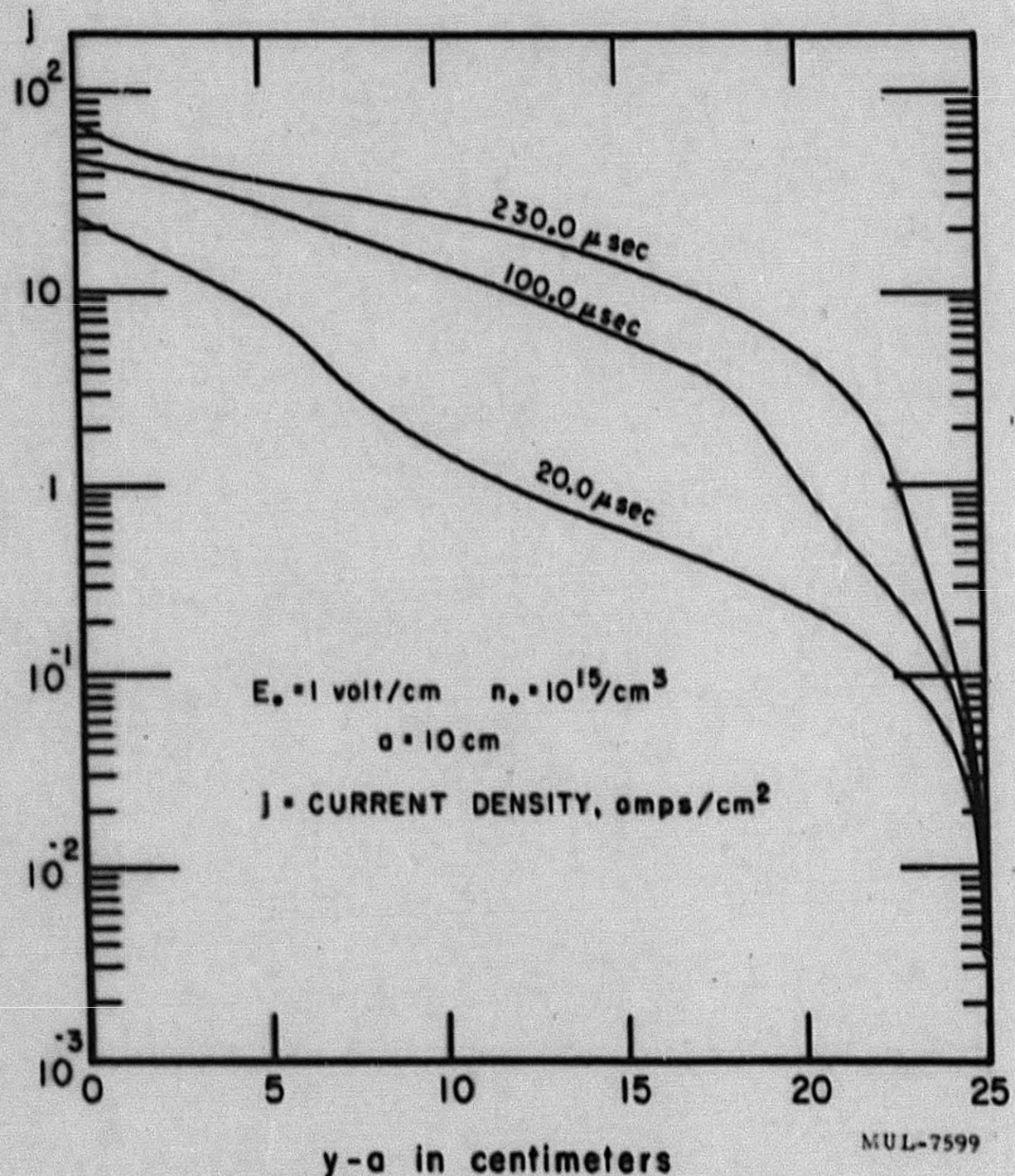

Fig. 16. Current densities at successive times.

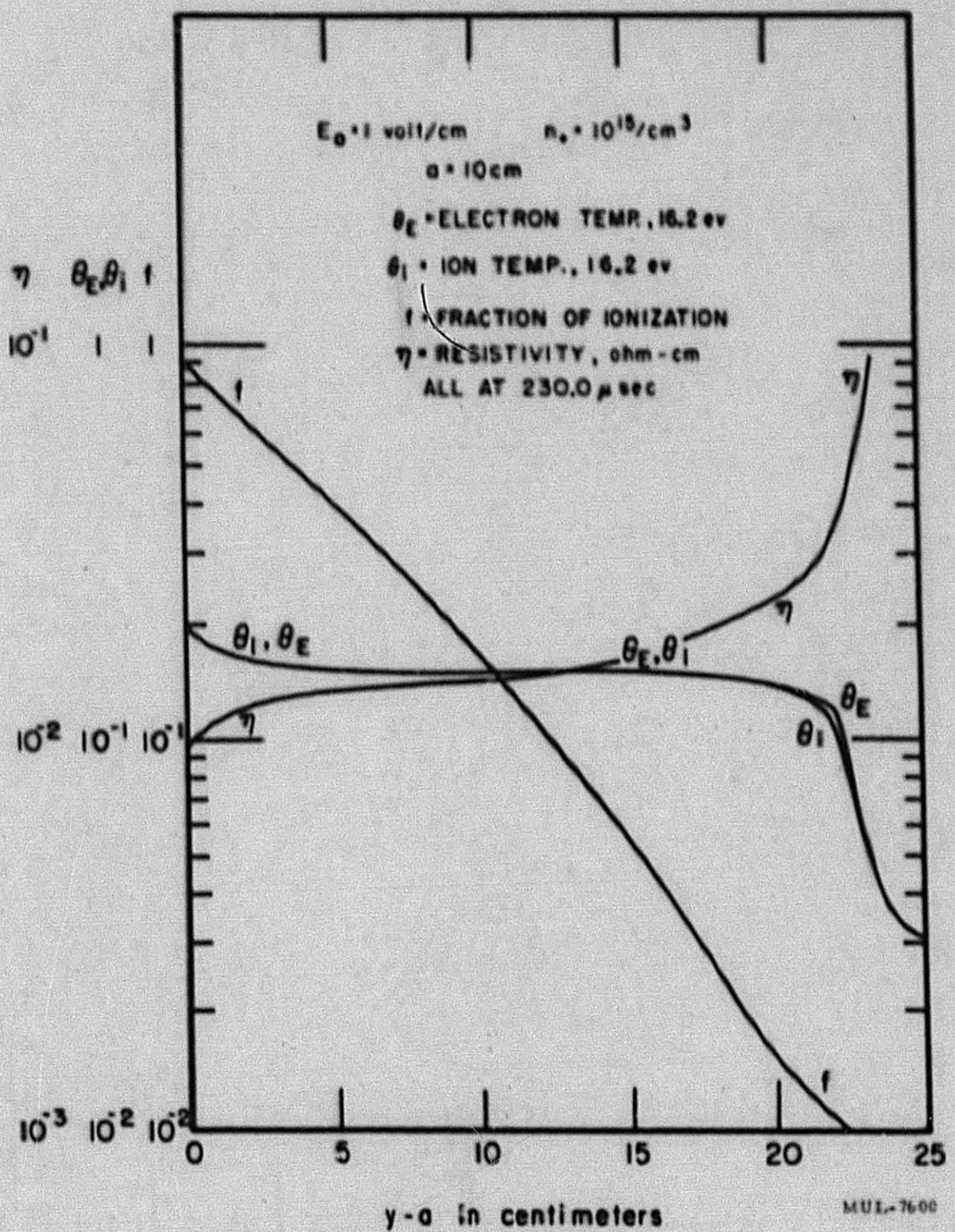

Fig. 17. Spatial distribution of plasma variables.

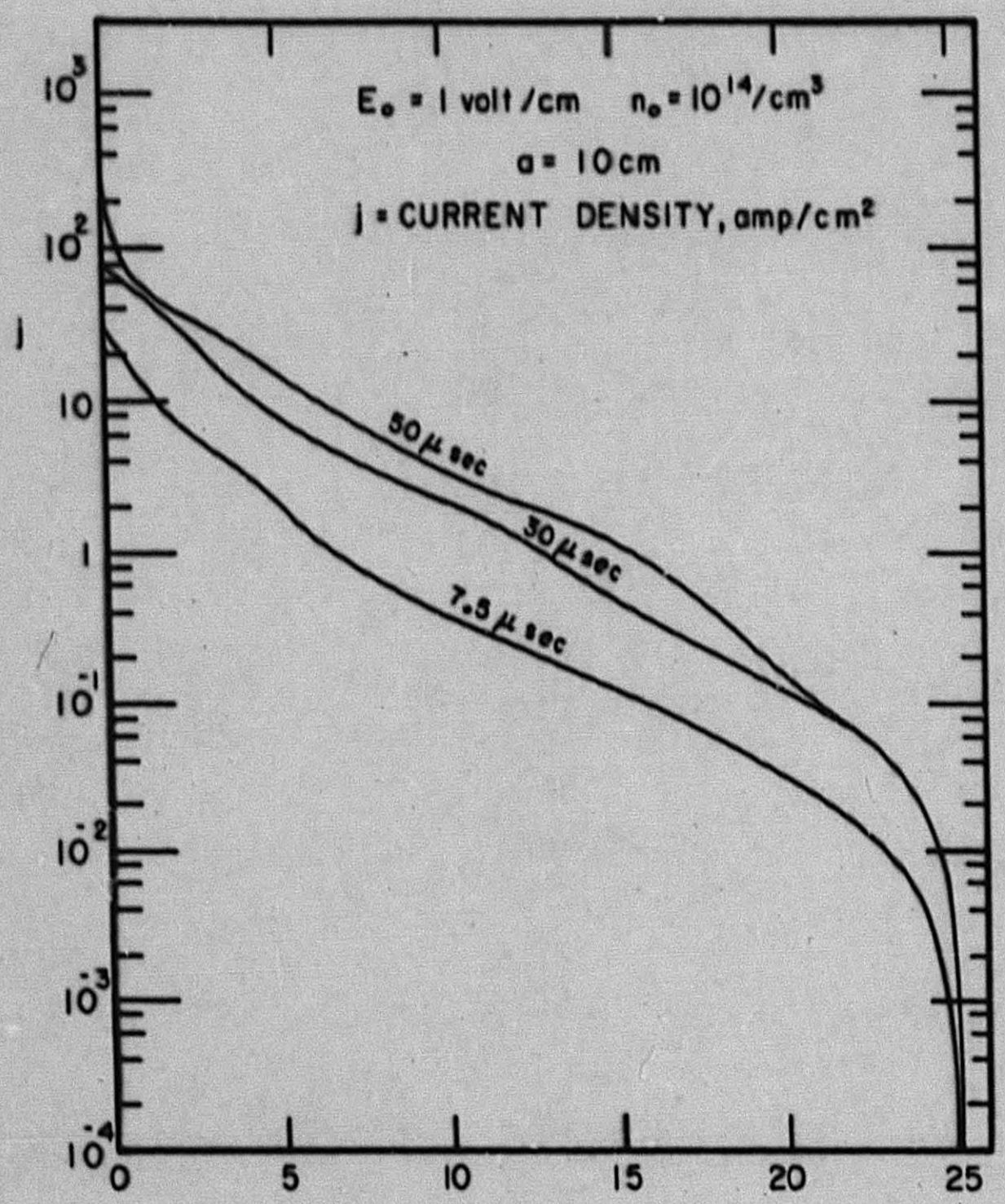

Fig. 18. Current densities at successive times.

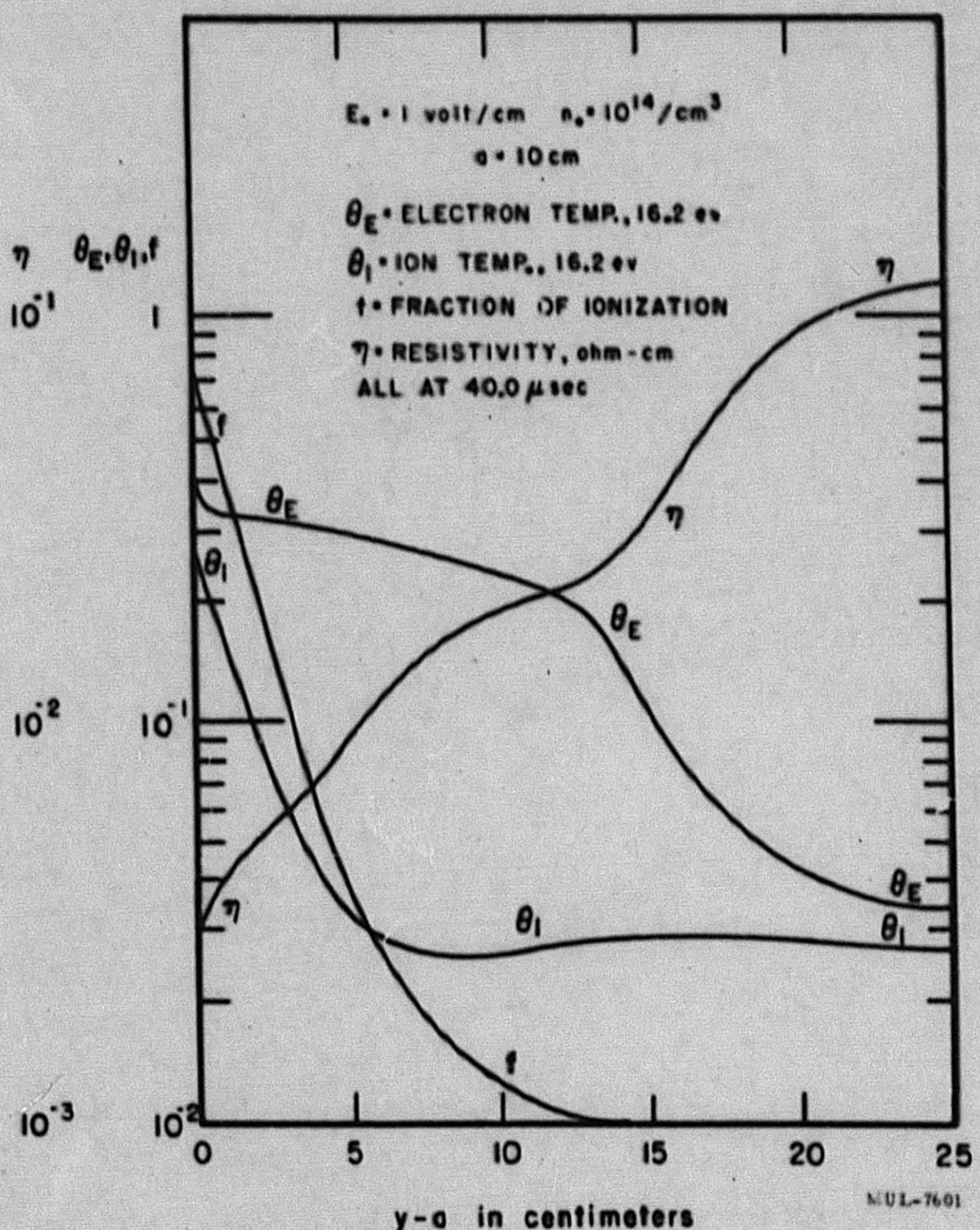

Fig. 19. Spatial distribution of plasma variables.

END